

---

EFDA–JET–CP(04)07-09

F. Crisanti, A. Becoulet, B. Esposito, C. Gormezano, F. Rimini, M. Brambilla,  
P. Buratti, A. Cardinali, M. de Baar, E. de la Luna, P. de Vries, X. Garbet,  
E. Giovannozzi, C. Giroud, R. Guirlet, E. Joffrin, X. Litaudon, P. Mantica,  
M. Mantsinen, A. Salmi, C. Sozzi, D. Van Eester and JET EFDA Contributors

# JET RF Dominated Scenarios and Ion ITB Experiments with Low External Momentum Input



# JET RF Dominated Scenarios and Ion ITB Experiments with Low External Momentum Input

F. Crisanti<sup>1</sup>, A. Becoulet<sup>2</sup>, B. Esposito<sup>1</sup>, C. Gormezano<sup>1</sup>, F. Rimini<sup>2</sup>, M. Brambilla<sup>3</sup>,  
P. Buratti<sup>1</sup>, A. Cardinali<sup>1</sup>, M. de Baar<sup>4</sup>, E. de la Luna<sup>5</sup>, P. de Vries<sup>6</sup>, X. Garbet<sup>2</sup>,  
E. Giovannozzi<sup>1</sup>, C. Giroud<sup>6</sup>, R. Guirlet<sup>2</sup>, E. Joffrin, X. Litaudon<sup>2</sup>, P. Mantica<sup>7</sup>,  
M. Mantsinen<sup>8</sup>, A. Salmi<sup>8</sup>, C. Sozzi<sup>1</sup>, D. Van Eester<sup>9</sup> and JET EFDA Contributors\*

*Associazione EURATOM-ENEA, IT*

<sup>2</sup>*Association EURATOM-CEA*

<sup>3</sup>*Association EURATOM-IPP, DE*

<sup>4</sup>*Association EURATOM-FOM, NL*

<sup>5</sup>*Asociacion EURATOM-CIEMAT, ES,*

<sup>6</sup>*EURATOM-UKAEA Fusion Association*

<sup>7</sup>*Associazione EURATOM-ENEA-CNR*

<sup>8</sup>*Association EURATOM-VR, SE*

\* See annex of J. Pamela et al, "Overview of JET Results",  
(Proc.20<sup>th</sup> IAEA Fusion Energy Conference, Vilamoura, Portugal (2004)).

Preprint of Paper to be submitted for publication in Proceedings of the  
20th IAEA Conference,  
(Vilamoura, Portugal 1-6 November 2004)

“This document is intended for publication in the open literature. It is made available on the understanding that it may not be further circulated and extracts or references may not be published prior to publication of the original when applicable, or without the consent of the Publications Officer, EFDA, Culham Science Centre, Abingdon, Oxon, OX14 3DB, UK.”

“Enquiries about Copyright and reproduction should be addressed to the Publications Officer, EFDA, Culham Science Centre, Abingdon, Oxon, OX14 3DB, UK.”

## ABSTRACT.

Advanced Tokamak scenarios include two different regimes: the “steady state” (characterized by the presence of an Internal Transport Barrier (ITB) ) and the “hybrid scenario” (characterized by central  $q > 1$  and a large region with magnetic shear close to zero). So far both the regimes, at least for the ion species, have always been obtained in presence of strong injection of external momentum by Neutrals Beam Injection (NBI) heating. By using Lower Hybrid Current Drive (LHCD) to sustain the central  $q$  slightly above one and with a large plasma region having the magnetic shear  $s$  close to zero, an “hybrid scenario” has been established, for the first time, in discharges with dominant Ion Cyclotron Resonance Heating (ICRH) and with a normalized beta close to two. By starting from a configuration with reversed magnetic shear (sustained only by LHCD) and with a well established ITB on the electron species, an ITB also on the ions species has been obtained by using ICRH in an ion minority heating scheme, ( $^3\text{He}$  )D. No external momentum input was provided by the NBI, except for the diagnostic charge-exchange and the MSE beams. In these discharges the evaluated ExB shearing rate was always very small (in the noisy range) and lower than analytical evaluations of the turbulence growth rate.

## 1. INTRODUCTION

So called “Advanced Tokamak Scenarios” usually refers to either of the following two different plasma regimes: “steady state” and the “hybrid scenario”. In both these regimes good performances have been achieved in several machines (JET, DIII-D, JT-60U, AUG), and a quasi steady state high value of the merit parameter  $H\beta_N$  has been obtained [1,2,3,4,5]. The two configurations are mainly characterised by two different types of current density profile. In “hybrid scenarios” [6] the central  $q$  is above one and a large central region is characterised by a magnetic shear  $s \sim 0$ . The so-called “steady state” scenario is characterized by a non-monotonic  $q$ -profile, compatible with large bootstrap current fraction, where in some condition ITBs are very often formed [1,7]. The value of minimum  $q$  is generally larger than two, and the ITB appears in the region with magnetic shear negative or close to zero. However the two regimes, when regarding the ions, have the common feature of having been obtained in the presence of strong injection of an external momentum by Neutral Beam Injection. So far the physics mechanism ruling the “hybrid scenario” is not clear. No sawtooth behaviour is present in the plasma centre ( $q > 1$ ), where, instead, a fish-bones activity is often going on. The plasma edge is characterised by the presence of a strong pedestal pressure and by the presence of ELMs (Edge Localised Mode) of type I. So far it is not clear whether the transport properties of these configurations are mainly due to the H mode feature or if some energy transport improvement also affects the plasma bulk. On the contrary, there are numerous experimental evidences and theoretic analysis showing that the ExB shearing rate may play the key role in stabilising the Ion Temperature Gradient (ITG) modes and in allowing the onset of an ITB on both the electron and ion species. However, it has been also shown by several experiments (JET, JT-60U, FTU, Tore Supra, AUG, TCV [9-14]) that an ITB on the electron species can be obtained

without any input of an external momentum, at the condition of having in the plasma centre region a negative magnetic shear. Two different kinds of experiments have been lately performed on JET and will be presented in the following. a) The “hybrid scenario” has been, for the first time, obtained in discharges with dominant ICRH at low  $\rho^*$  ( $\sim 3.5 \times 10^{-3}$ ) and with the current profile sustained by using a LHCD: with this heating scheme the effect of  $T_i/T_e$ , in principle, can be studied. Eventually, in this configuration a limited  $\beta_N$  has been achieved. b) An ion ITB has been obtained by using the ICRH in an ion heating scheme, ( $^3\text{He}$ )D, and without any NBI, except the diagnostic beams, in discharges with a well developed electron ITB in presence of reversed q profile.

## 2. RF DOMINATED “HYBRID SCENARIO”.

To perform these experiments, a pulse design similar (current and power waveforms) to the one used for the development of standard JET hybrid scenarios [6] was selected. Instead of trusting only on the heating timing and on some MHD behaviour (like fishbones), the current density profile was kept under control by using a proper LHCD in the prelude phase and by maintaining the LH power during the steady state phase. Operating in such a way large flat shear profiles, with q slightly larger than 1, have been established and sustained for several seconds. The experiments here presented [8] were all performed at fixed toroidal field ( $B_T = 3.2 \text{ T}$ ), whilst the plasma current was varied, in several steps, between 1.9 MA and 2.6 MA ( $3.5 < q_{95} < 6$ ). The central electron density varied between  $2.5 < n_e(0) < 4 \cdot 10^{19} \text{ m}^{-3}$ . Typically the ICRH power was of the order of 10 MW, whilst the NBI power was varied between 0 and 10 MW, to explore the role of the external added momentum input. A typical scenario is shown in Fig. 1 for a case with  $P_{\text{RF}} \approx P_{\text{NBI}}$ . In the experiments performed with pure RF heating the stored energy increased continuously during the pulse with  $H_{89}$  and  $\beta_N$  reaching respectively 2.2 and 1.2. About 1.5 MW of LHCD were used during the current rise and maintained during the high power phase to sustain the q profile. The ion temperature profile was not available in these experiments (for the absence of the diagnostic NBI beam), but  $T_i/T_e \approx 0.8$  it has been estimated. The ion temperature indicated in Fig.1 is given by the X-ray crystal spectrometer and it located at  $r/a$  between 0.2 and 0.4. A common feature is the very low ELM activity (in pure RF heating the discharges remained always in L-mode), although the total injected power was about 3 times the L-H threshold power. The q profile, as obtained by the equilibrium code (EFIT) constrained by the Motional Stark Effect data (MSE), was slightly above one and with the magnetic shear close to zero on a large plasma region. In the central region of these discharges magnetic oscillations (Fig. 2) with toroidal number  $n=1$  and constant or slightly increasing frequency below 7 kHz are very often present [15]. During mode growth the electron temperature decreases around the plasma center and increases outside an inversion radius. This evolution resembles a sawtooth collapse, but it is much slower (300 ms in the present “slow sawtooth” case, less than 1 ms in an ordinary one). All these discharges have NTM activity with  $n=2$  or  $n=3$ . Neoclassical tearing modes with  $m/n=3/2$  appear before the onset of  $\dot{\theta}$  slow sawteeth and saturate at small amplitude [16].  $H_{89} \times \beta_N / q_{95}^2$ , versus the total injected power, is reported in Fig.3 for three different sets of  $q_{95}$

values. The maximum achieved values are of the order of 0.2, below the values of 0.4 achieved in JET at higher  $\rho^*$  and comparable with the ones of standard Scenario at similar  $B_T$ . However these performances were not limited by MHD events, but by the lack of available power. In addition, a possible reason for this relatively low value of  $H_{89}xb_N/q_{95}^2$ , might be linked to the low value of the pressure pedestal compared with the NBI dominated hybrid scenarios. The thermal energy reaches values close to  $H_{98y}^2=1$  [8] for the best discharge, but with type III ELMs and with a very low edge pedestal pressure that remains constant with the injected power up to the highest stored energy ( $\sim 4.5$  MJ). Another important issue to underline is the quality of the temperature gradients. The experimental values of the normalized gradient  $R/L_{Te}$  ( $L_{Te}=T_e/[dT_e/dr]$ ) in these experiments ranged between 8 and 10, being pretty similar to the one of the standard JET “hybrid scenarios”. This range of normalized gradient values, although smaller of the ITB ones, is comparable or larger than the values achievable in the standard H mode experiments. The achieved  $b_N$ , in these low  $\rho^*$  discharges, is shown in Fig.4 in comparison with the data achieved in other experiments [5]. There is a domain, typically with  $\rho^*>7\cdot 10^{-3}$ , for which  $\beta_N$  is limited by MHD events. For lower values of  $\rho^*$ , typical of high field JET experiments,  $\beta_N$  is clearly limited by the available power. In particular the figure points, representing the experiments here described, are the ones with  $P_{TOT}$  ranging between 16 and 20 MW ( $P_{RF} \approx P_{NBI}$ ), consequently a strong increase of ICRH power is necessary to explore the beta limits in such kind of experiments.

### 3. ITB WITHOUT MOMENTUM INJECTION.

Quasi steady state electron ITBs, without any input of external momentum, are routinely obtained in JET plasmas by using the LHCD to sustain a reversed q profiles [9,1]. So far the electron heating transport of these discharges was studied by using the ICRH in low concentration H minority scheme. In order to explore if the physics behind the electron ITB is the same of the more common ion ITBs, we projected the following experiment. An electron ITB scenario, with reversed magnetic shear, was used in the attempt to heat the bulk ions without any external momentum input, by using the ICRH in a  $^3\text{He}$  minority scheme. A reference discharge with  $B_T=3.45\text{T}$ ,  $I_p=2.5\text{MA}$ ,  $\langle n_e \rangle \sim 2.0 \cdot 10^{19}\text{m}^{-3}$ ,  $q_{95}=4.5$  was selected. An electron ITB was sustained up to a length  $\tau_{de} \sim 8$  s by using about 2MW of LHCD to control a reversed q profile, where  $q_{min}$  varied along the discharge between 4 and 2. Up to 6 MW of ICRH at 37 MHz were coupled to the plasma. The optimal minority concentration was carefully selected by using different ICRH coupling codes. In particular we have used the 2D full wave TORIC code (taking in account the real JET geometry) and a Fokker/Planck code, coupled with TORIC, to evaluate the coupling of the fast  $^3\text{He}$  ions to the bulk ions and electrons [17]. With a minority fraction of the order of 4%, it is found that about 80% of the coupled power goes to the  $^3\text{He}$  ions; out of this power fraction something of the order of 60% is then transferred to the majority ions by collisions. Eventually, a maximum of about 50% of the injected ICRH power can be coupled to the bulk ions. This result was cross-checked by varying the minority concentration in several discharges where the ICRH power was modulated to find the power fraction

coupled with any species. The time waveforms of the keys quantities are shown in Fig. 5 for the discharge #62607, in which the used  $^3\text{He}$  concentration was slightly higher than the optimum 4% value. About 2 MW of NBI power was used for measuring the ion temperature and the MSE angle. In order to minimise NBI input, the NBI power was modulated (Fig. 5). The fact that a low external momentum was nevertheless injected will be re-discussed later on. In total, less than 8 MW were coupled to the plasma with about 4 MW coupled to the ions. An ion heating was always evident whenever a suitable  $^3\text{He}$  concentration was used. In the early phase of the ICRH application an electron transport barrier was always present at half plasma radius, see the maximum of  $r_{\text{Te}}^*$  in Fig.5, (here  $\rho_{\text{Te}}^*$  [18] characterises the presence and the strength on an ITB). Around  $t=46\text{s}$  this barrier shrank in radius but never disappeared. When the  $^3\text{He}$  was optimized and the ICRH power was the maximum available, an ion ITB was sometime also observed during this phase. However, the most interesting feature of the experiment is the transient onset of an ion barrier, and a strengthening of the electron one, around  $t=48.5\text{s}$ . This effect, that can be noted in the central  $T_i$  and  $T_e$  signals and in the  $\rho_{\text{Te},i}^*$  traces in Fig. 5, was always present (with different strength) whenever sufficient ion heating was applied: by varying the  $^3\text{He}$  concentration, the ion heating was varied from a fraction close to zero up to the maximum 50%, previously mentioned. Always in Fig. 5, the time behaviour of the  $q$  value (as measured by the polarimetry at the radius  $R \approx 3.1\text{ m}$ ) is also shown. Such measurement has been compared and verified, in a couple of different time slices, with the  $q$  profile obtained by using the MSE data and equilibrium code EFIT. It is very interesting to note that, around the time when the barrier on the ions appears, the  $q$  is crossing the value of 2. Moreover, always around that time, the  $q$  profile in the central region is no longer reversed; consequently the magnetic shear is no longer negative and a large region with a magnetic shear close to zero appears in the plasma. The evolution of the ion temperature and of the toroidal rotation profiles is reported in Fig. 6a,b for three different times. At  $t = 48.5\text{s}$  the ion temperature increases in the central region and a clear discontinuity in the profile derivative is present at  $R \approx 3.3\text{m}$ ; in this region the normalized temperature gradient parameter achieves the value  $R/L_{T_i} \sim 15$  and the ITB parameter  $\rho_{T_i}^* \sim 1.5 \times 10^{-2}$  (above the standard threshold:  $\rho_{T_i}^* \sim 1.4 \times 10^{-2}$ , Fig.5). Although, as previously already mentioned, a very low input of external momentum was always injected for diagnostic purpose, the measured toroidal rotation was quite small at any time ( $< 30 \times 10^3\text{ rad/sec}$ , close to the measurements noise) and no momentum transport barrier was observable, at least inside the diagnostic capability. This can be noticed in Fig.6b, where the profile of the toroidal rotation is shown for three different times. For comparison we show also the profile of the toroidal rotation for a typical JET ITB discharge [19]. In such typical ITB discharge both the central ion temperature and the total injected power were about a factor three larger, whilst, in the present experiments, the toroidal rotation is around a factor 15 smaller. The ExB shearing rate, as evaluated by using the neo-classical theory to infer the poloidal velocity, was always very low ( $\omega_s < 30 \times 10^3\text{ rad/sec}$ ) and in any case very close to the measurements noise. Moreover  $\omega_s$  was of the same order of magnitude as the ITG linear growth rates estimated both in the ballooning approximation and in



the rational  $q$  density approximation [20]. This can be observed in Fig.7b, where the shearing rate and the ITG linear growth rates are shown, versus time, at fixed plasma radius ( $R=3.25\text{m}$ ). Again, as a reference,  $w_s$  is also shown for a standard JET ITB. In the same figure (Fig.7a) the ion thermal diffusivity  $\chi_i$ , as inferred from by the experimental data by using the transport code JETTO, is also shown. It is pretty evident a thermal diffusivity collapse occurs at  $t \approx 48.5\text{s}$  when, in the high gradient region ( $3.0\text{m} < R < 3.3\text{m}$ ),  $0.4 < \chi_i < 1.0 \text{ m}^2\text{s}$ . To evaluate the performances of these ITBs with no, or very low, external momentum input, in Fig.8 we report  $\beta_N$  versus the total injected power for a pulse data set representing all the JET ITB scenarios with similar toroidal field. Looking at this plot a substantial point must be kept in mind. In the discussed case the coupled LHCD power (essentially current drive) is  $\approx 20\%$ , comparable with the NBI power; moreover the power coupled to the ions is only around 40% of the total. The discharge with no external momentum input is located just in the middle of the cloud of points; consequently, although any kind of extrapolation is always arbitrary, we might expect a strong increase of the achieved  $\beta_N$  by increasing the ion heating power. In order to have some comparison with other experiments in different scenarios, with and without external momentum injection, we have inserted the achieved value of  $b_N$  in Fig.4 (marked with the pulse number #62798), where this quantity is plotted versus  $\rho^*$ . Again, keeping in mind the very low power coupled ( $\approx 4\text{MW}$  respectively to the ions and to the electrons), it is surprising how such discharge is close to all the other points.

#### 4. DISCUSSION.

Experiments, with small or negligible external momentum input, have been performed in two very different “Advanced Scenario” plasmas. So far it is not yet evident whether the improved transport properties of the so called “hybrid regime” are essentially due to the good quality of the pressure pedestal, or if also the plasma bulk is characterised by good confinement qualities. In the “hybrid” experiments here described good performances have been obtained with the plasma edge in L mode or with a tiny ELM III activity. Unfortunately, with the performed experiments, it is not yet possible to give a final answer to the transport problem, mainly because some essential experimental profiles (e.g. that of the ion temperature) were not always available and the plasma edge was not well characterised. A strong similarity with quite different experiments (FTU, Tore Supra, TCV [11,12,14]) has been widely discussed in a previous paper [8]; however, here it is worth to mention that in all these experiments the good performances have always been obtained with a  $q_{\min}$  slightly higher than one and with a large region of magnetic shear close to zero or slightly reversed; moreover, also in all these experiments no external momentum was injected. This latter point is also the link with the second type of experiments here presented. In this second case the plasma scenario was a typical JET ITB configuration with a target  $q_{\min}$  larger or equal to 2 and with a negative magnetic shear in the central region. Usually, in a well developed ion ITB, a strong ExB shearing rate is present in the plasma and it is thought to be the main turbulence stabilizing factor. However, so far, it is not yet clear whether this sheared flow is also the trigger of the turbulence reduction. In our

experiment we have observed that, once an electron barrier is well developed in a reversed magnetic shear configuration, an ion ITB can be created by only heating the bulk ions and without external momentum input, and, more important, with a very negligible shear flow. Unfortunately, the good confinement phase, although very repetitive, was always transient. With the available data it was not possible to understand exactly the reason of this phenomenology. For sure the absence of substantial levels of auxiliary heating (only less than 3MW of ICRH coupled to the ions) did not enable to obtain very strong ITBs. Moreover, for technical problems, we were not able to vary the target  $q$  profile, and, consequently to study the dependence of the observed phenomenology on this key parameter. Another very important problem that we did not explore (again for the lack of power) was the dependence on the NBI (external momentum) injected power. In any case a possible explanation of the observed phenomenology could be (at least at the available additional power level) that a negative magnetic shear (with a small  $s=0$  region), by itself, is not sufficient for the onset of an ion ITB; the appearance of a rational  $q$  surface can further reduce the turbulence growth rate, facilitating the transition. For all these reasons we are planning to repeat this experiment during the upcoming JET experimental campaigns, when, having installed the new ICRH antenna, more RF power will be available. Let us now come back on the only common feature between the two different scenarios described above: the presence of a region with a magnetic shear  $s\sim 0$  [20]. Whilst this can be invoked to justify the ITB onset [20], it seems difficult to correlate it with the “hybrid regime”, as the large temperature gradient region is much larger than the  $s\sim 0$  region. For this reason, we believe that some more accurate turbulence analysis should be performed to explore whether this common feature can be also used as a common justification or if two different mechanisms are behind the two phenomena.

## REFERENCES.

- [1]. Challis, C., et al., “The use of transport barriers inside tokamak plasmas”, 31st EPS, London 2004, I1-02.
- [2]. Luce, T.C., et al., “High performance stationary discharges in the DIII-D tokamak”, *Phys. Plasmas* **11** (2004) 2627.
- [3]. Isayama, A., et al., *Nuclear Fusion*, 41, 2001, 761.
- [4]. Isayama, A., “Steady state High-beta Experiments in JT-60U Hybrid Experiments”, presented at the ITPA meeting, Naka March 2004.
- [5]. Sips, A.C., et al., “Improved-H mode identity experiments in JET and ASDEX Upgrade”, 30th EPS, St.Petersburg 2003, O-1.3A.
- [6]. Joffrin, E., et al., this Conference
- [7]. Connors, J.W., et al., “A review of internal transport barrier physics for steady-state operation of tokamaks”, *Nucl. Fusion* **44** (2004) R1-R49
- [8]. Gormezano, C., et al., “Hybrid advanced scenarios: Perspectives for ITER and experiments with dominant RF heating”, 31st EPS, London 2004, I5-01.

- [9]. Hogewei, G.M.D., et al., “Electron Heated Internal Transport Barrier in JET”, *Plasmas Phys. Control. Fusion* **44** (2002) 1155.
- [10]. Fujita, T., et al., “High performance experiments in JT-60U reversed shear discharges”, *Nucl. Fusion* **39** (1999) 1627.
- [11]. Pericoli R, V., et al., “Progress towards internal transport barriers at high plasma density sustained by pure electron heating and current drive in the FTU tokamak”, *Nucl. Fusion* **43** (2003) 469.
- [12]. Hoang, G.T., et al., “An H minority heating regime in Tore Supra showing improved L mode confinement”, *Nucl. Fusion* **40** (2000) 913.
- [13]. Wolf, R.C., et al., “Performance, heating and current drive scenarios of ASDEX Upgrade advanced tokamak discharges”, *Nucl. Fusion* **41** (2001) 1259.
- [14]. Pietrzyk, Z.A., et al., “Long-Pulse Improved Central Electron Confinement in the TCV Tokamak with Electron Cyclotron Heating and Current Drive”, *Phys. Rev. Letters*, **86** (2001) 1530.
- [15]. Buratti, P., et al., “Observation of slow sawtooth reconnection in JET low-shear plasmas”, 31st EPS, London 2004, P1-165.
- [16]. Belo, P., et al., “Observation and implication of MHD modes for the hybrid scenario”, 31st EPS, London 2004, P1-170.
- [17]. Brambilla, M., “Quasi-linear ion distribution function during ion cyclotron heating in tokamaks”, *Nucl. Fusion* **34** (1994) 1121.
- [18]. Tresset, G. et al., “A dimensionless criterion for characterizing internal transport barriers in JET” *Nucl. Fusion* **42** (2002) 520.
- [19]. Crisanti, F., et al., “JET Quasistationary Int.-Transp.-Barrier Operation with Active Control of the Pressure Profile”, *Phys. Rev. Letters*, **88** (2002) 145004.
- [20]. Esposito, B., et al., “JET internal transport barriers: experiment versus theory”, *Plasmas Phys. Control. Fusion* **45** (2003) 933.

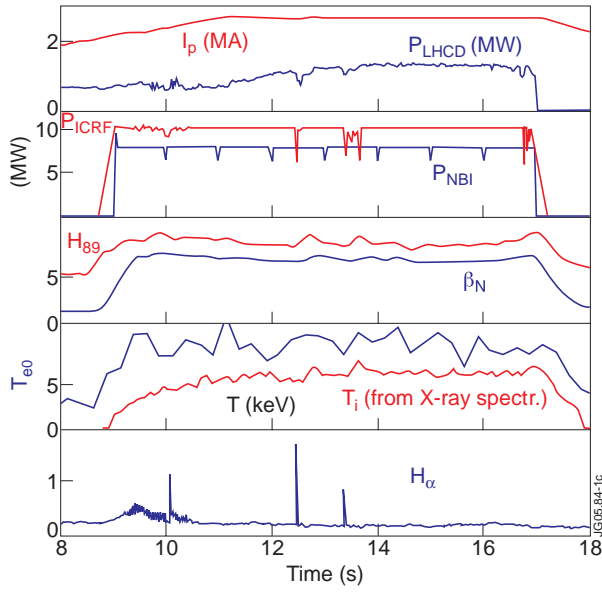


Figure 1: Main signals for an RF dominated “hybrid scenario” in JET (Pulse No: 62789,  $q_{95}=3.8$ ).  $T_i$  from X-ray spectrometer, given at about  $0.4 r/a$  ( $T_{i0}=0.8T_{e0}$ ). Note the absence of any strong ELM activity.

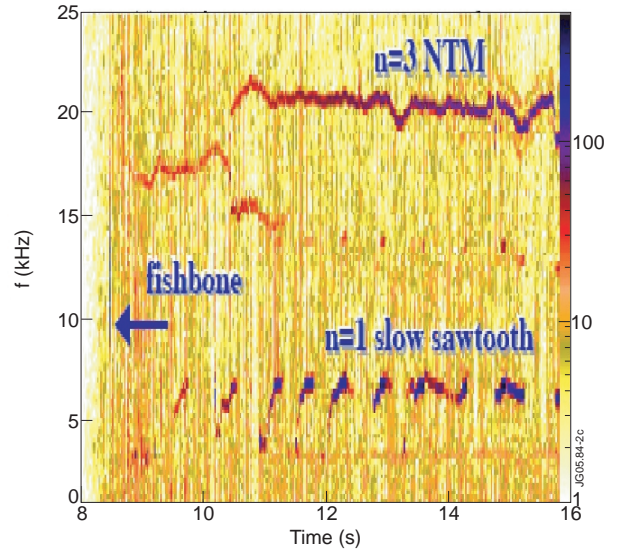


Figure 2: Pulse No: 62779. Spectrogram of magnetic oscillations below 25kHz. Bursts between 4 and 7kHz are  $n=1$  slow sawteeth. The line near 20kHz is an  $n=3$  NTM. The intense, almost vertical line at  $t=8.6$  s is a fishbone.

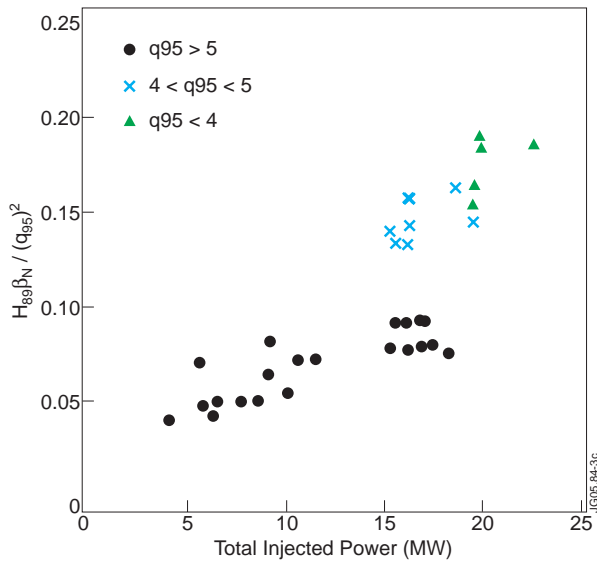


Figure 3:  $H_{89}\beta_N/q_{95}^2$ , versus the total injected power, divided in three different sets of  $q_{95}$  values.  $B_T=3.2T$

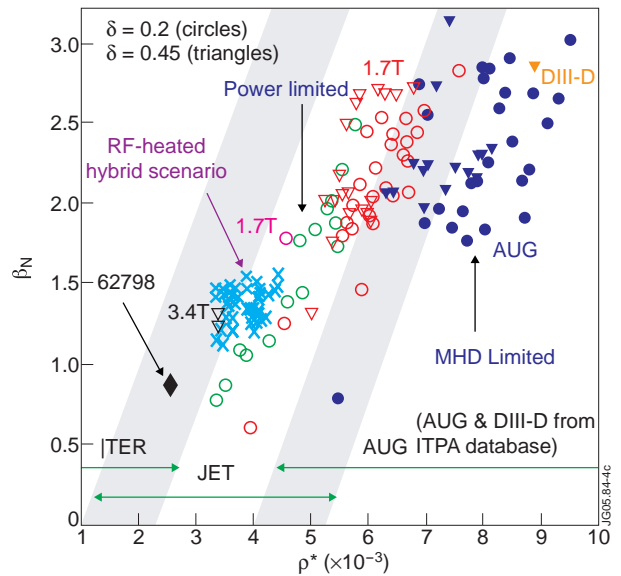


Figure 4: Database for  $\beta_N$  versus  $\rho^*$ . New data from RF dominated “hybrid” scenarios are not MHD limited. The Pulse No: 62798 indicates the ITB performance without momentum injection.

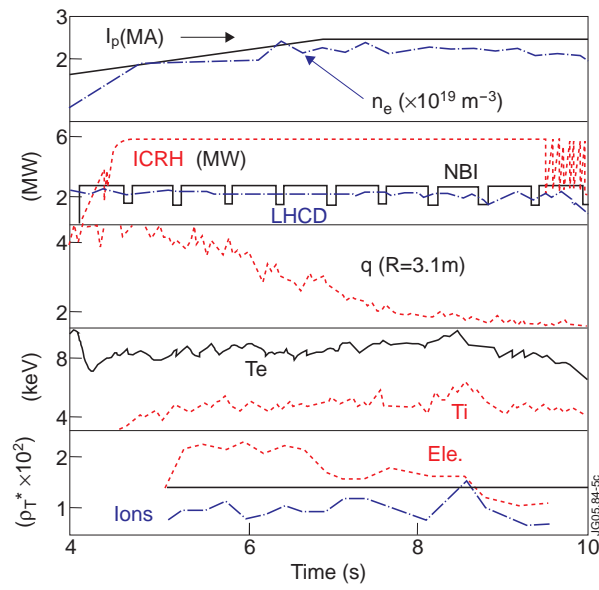


Figure 5: Main signals for Pulse No: 62607 ( $B_T = 3.2T$ ).

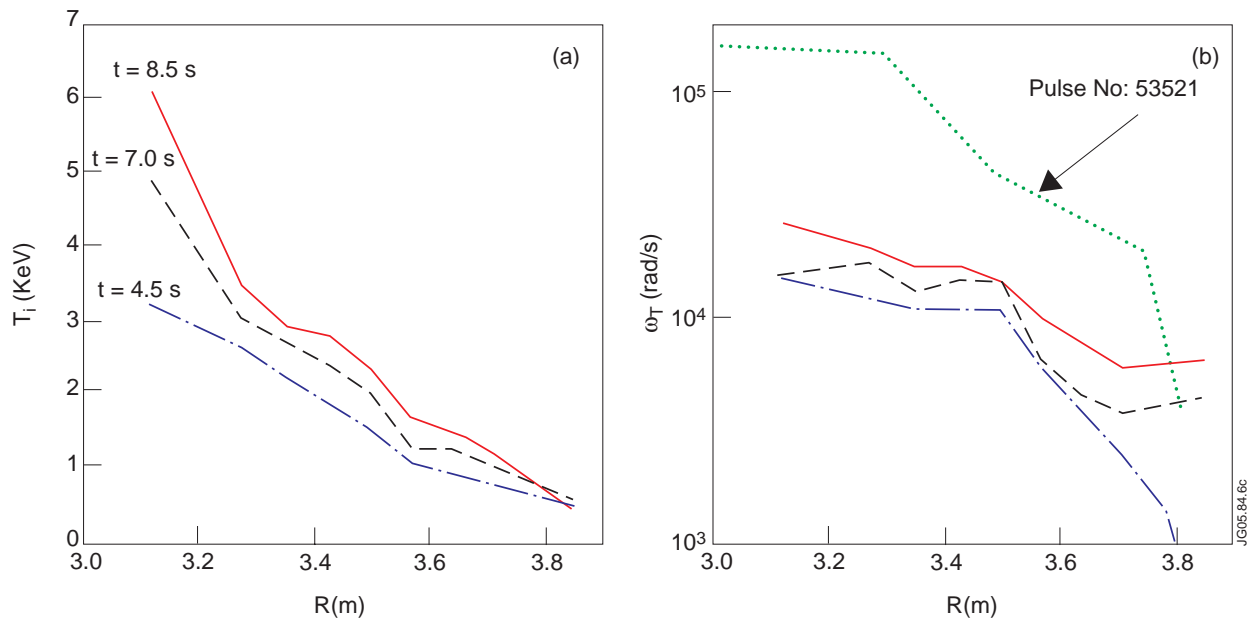


Figure 6: Pulse No: 62607. a) Ion temperature profile at three different times b) Toroidal rotation profile at the same times of the temperatures; with the Pulse No: 53521 it is indicated the typical rotation in a JET ITB.

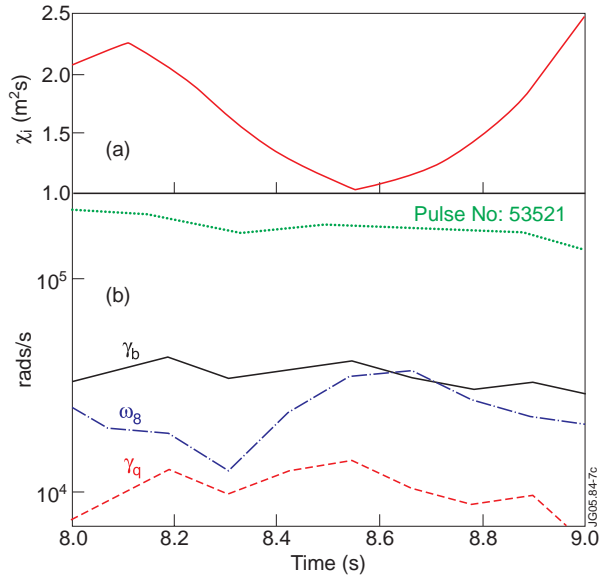


Figure 7: Pulse No:62607. a) The ion thermal diffusivity,  $\chi_i$ , versus time at fixed plasma radius. b) The  $E \times B$  shearing rate ( $\omega_s$ ) and two different evaluation of the ITG linear growth rate ( $\gamma_b$ ,  $\gamma_q$ ); with the Pulse No:53521 it is indicated the typical shearing rate value in a JET ITB.

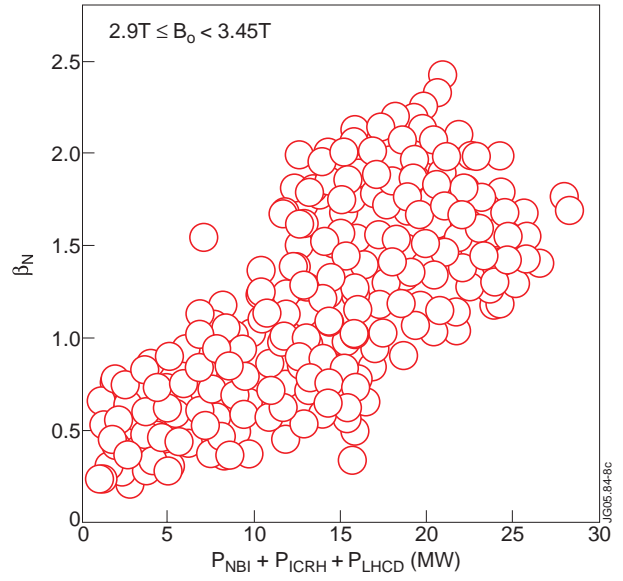


Figure 8:  $\beta_N$  versus the total additional power for the full dataset of JET ITB plus (black filled point, Pulse No: 62798) the ITB without external momentum injection.